LA-UR -85-2743

Los Alamos National Laboratory is operated by the University of California for the United States Department of Energy under contract W-7405-ENG-36.

TITLE: SHUTTERING EFFICIENCIES OF NANOSECOND-GATED PHOTOEMISSIVE SHUTTER TUBES

LA-UR--85-2743

DE85 015728

AUTHOR(S): George J. Yates and Steven A. Jaramillo
Thomas S. Pagano and J. Paul Black

SUBMITTED TO: 1985 SPIE
San Diego, CA
August 19-23, 1985.

Los Alamos

Los Alamos National Laboratory
Los Alamos, New Mexico 87545

FORM NO. 836 R4
ST. NO. 2629 5/81

Shuttering efficiencies of nanosecond-gated photoemissive shutter tubes

George J. Yates and Steven A. Jaramillo

Physics Division, University of California, Los Alamos, National Laboratory
Group P-15, Mail Stop D406, P.O. Box 1663, Los Alamos, New Mexico 87545

and

Thomas S. Pagano and J. Paul Black

EG&G Inc., Energy Measurements Division
Santa Barbara Operations and Kirtland Operations

Abstract

Recent studies show that effective shuttering of photoemissive tubes, such as Silicon-Intensified-Target Vidicons (SITVs) and Microchannel-plate Image Intensifier Tubes (MCPTs), can vary widely depending upon the extent of their opacity to an input flux of photons. Optical feedthrough signals from photon transmission through the photocathode to the target or phosphor ranging from 10^{-4} to 10^{-9} (when compared with gated signals) were measured for a large sampling of commerically available units. Effective shutter ratios of 10^5 to 10^8 measured for units operated in quiescently dark environments can be substantially reduced by optical feedthrough. Furthermore, ineffective suppression of photoemission can cause further reductions in shutter ratio. Reductions are roughly correlated with the ratio of optical gate duration to light pulse duration. Experimentation with various thicknesses of aluminum depositions on MCPT phosphors and chromium layering on SITV silicon targets indicate substantial reductions (2x to 15x) in transmission with minimal increases in threshold voltages required for gain. These results, together with exploratory studies of external coating of output fiber optics with transmission filters spectrally matched to minimize feedthrough to P-20 phosphors are reported.

Introduction

In many applications these shutter tubes are exposed to transient optical scenes that vary in intensity over a 10^5 to 10^6 dynamic range and persist several orders of magnitude longer than the shutter period. To linearly record the image intensity at various times throughout such light impulses requires fast shutter gate response and an extinction ratio outside the optical gate of greater than 10^6. For this type of shutter, two shutter ratios exist: (1) photon shutter ratio caused by the unintended transmission of input flux from the photocathode to the target and (2) electron shutter ratio which is the effectiveness of the reverse bias electric field in suppressing photocathode emission.

Earlier we reported[1] maximum dynamic or gated shutter ratios of $> 10^7$ for MCPTs and $\gtrsim 10^3$ for SITVs operated in a dark environment and stimulated with delta function impulses of light (500 ps FWHM light pulses time-phased to coincide with 5 ns optical gates). Refinements of those measurements show that shutter ratios also vary with (1) magnitude of reverse bias used for suppression of photocathode emission and (2) magnitude of MCP or SIT gain during gate time. These effects, combined with the integrated effects from optical feedthrough in field applications where these units are coupled to light sensitive devices (the silicon target for SITVs and film, Sb_2S_3 vidicons, CCDs, or CIDs for MCPTs) with broad spectral responses making it difficult to distinguish between signals produced from transmitted light and those produced from photoelectrons are discussed.

Opacity Measurements

We reported[1,2] photon shutter ratios for gated SITVs earlier. Recently we observed similar problems for MCPTs. The opacity for several samples was measured by using a broad-band CW lamp to illuminate the photocathode while monitoring the phosphor with a radiometer. The experimental set-up is shown in Fig. 1. The CW lamp (American Optical Model 265 with microscope lens) was located 6-1/2 inches from the MCPT photocathode. A 1-cm^2 circular aperture was used to mask the MCPT photocathode so that its illuminated area would be equal to the input aperture for the EG&G model 550 radiometer.

The light penetrating the phosphor was measured with the radiometer sampling head butted directly against the MCPT output fiber optic while the photocathode was exposed.

The optical energy of the CW lamp (labeled Input Energy in Table I) was measured at the MCPT photocathode plane by removing the MCPT and positioning the radiometer sensing head at the same location. A neutral density gelatin filter, ND 4.0, was inserted between the CW source and the radiometer to attenuate the input light to a level compatible with the dynamic range of the radiometer. The table entries are actual readings corrected upward by 10^4 to account for the series ND. The average optical power density was $\approx$ 200 mW/cm^2 for this data set. The wavelength spectrum, measured with a LI-COR model LI-1800 spectrometer is shown in Fig. 2. Essentially, what we are measuring by this method is the attenuation of visible light which occurs by having the MCPT in the light path. The Input/Output columns of Table I show the attenuation factor or optical shutter ratio for the MCPT. These attenuation data converted to equivalent transmission are Data Set I in Table II.

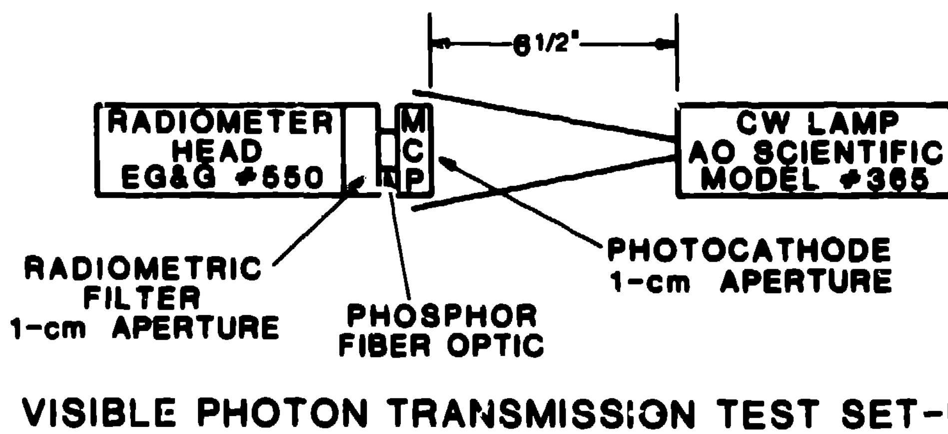

Fig. 1. The opacity measurement setup

Table I. MCPT optical attenuation factors

Manufacturer	SN	Input Energy (μJ/cm^2)	Feedthrough Energy (μJ/cm^2)	Input/Output
ITT	782/1	0.203×10^{4}	0.348×10^{-1}	0.59×10^{5}
"	871/1	0.183×10^{4}	0.767×10^{-2}	0.24×10^{6}
"	839/11	0.182×10^{4}	0.199×10^{-2}	1.10×10^{6}
"	787/1	0.222×10^{4}	0.246×10^{-1}	0.90×10^{5}
"	14-180/1	0.189×10^{4}	0.131×10^{-3}	1.44×10^{7}
"	14-180/17	0.193×10^{4}	0.239×10^{-1}	0.81×10^{5}
"	840/2	0.191×10^{4}	0.460×10^{-2}	0.42×10^{6}
"	849/6	0.188×10^{4}	0.139×10^{-1}	1.35×10^{5}
"	871/2	0.193×10^{4}	0.248×10^{-2}	0.78×10^{6}
"	839/19	0.176×10^{4}	0.660×10^{-2}	0.27×10^{6}
"	14-311/3	0.178×10^{4}	0.211×10^{-2}	0.84×10^{6}
"	883 5	0.177×10^{4}	0.077×10^{-3}	2.30×10^{7}
"	14-311/4	1.28×10^{3}	0.35×10^{-3}	3.7×10^{6}
VARO	409033	0.179×10^{4}	0.068×10^{-3}	2.40×10^{7}
"	409239	0.190×10^{4}	0.339×10^{-3}	2.39×10^{6}
"	409229	0.188×10^{4}	0.307×10^{-3}	6.12×10^{6}
"	403751	0.172×10^{4}	0.223×10^{-3}	0.77×10^{7}
"	415033	0.198×10^{4}	0.271×10^{-3}	0.73×10^{7}
"	401199	0.181×10^{4}	0.094×10^{-3}	1.93×10^{7}
"	70941	0.191×10^{4}	0.297×10^{-3}	0.64×10^{7}

Table II. MCPT and SITV optical transmission values

	MCPTs	Transmission Range
	3 ITT	0 to 4.9×10^{-7}
	1 ITT	5 to 9.9×10^{-7}
	8 ITT	0 to 4.9×10^{-6}
Data Set 1	2 ITT	5 to 9.9×10^{-7}
	1 ITT, 2 Varo	0 to 4.9×10^{-7}
	1 ITT	5 to 9.9×10^{-8}
	1 ITT, 3 Varo	0 to 4.9×10^{-8}
	2 Varo	0 to 4.9×10^{-9}
	MCPTs	**Transmission Range**
	Varo-1	5×10^{-7}
	Varo -2	1.3×10^{-7}
	ITT-1	2.5×10^{-5}
	ITT-2	1.4×10^{-5}
	Varian	2.5×10^{-6}
Data Set 2	Phillips	2.0×10^{-6}
	Delli Delti-1	3.0×10^{-7}
	Delli Delti-2	1.2×10^{-6}
	SITVs	
	EG&G-1	1.0×10^{-5}
	EG&G-2	6.0×10^{-6}
	MCPTs	**Transmission Range**
	2	0 to 4.9×10^{-4}
	1	5 to 9.9×10^{-5}
Data Set 3	6	0 to 4.9×10^{-5}
	3	5 to 9.9×10^{-6}
	2	0 to 4.9×10^{-6}

Independent measurements on eight new samples and two SITVs (phosphor targets in lieu of silicon) were taken at GE&G/SBO (Santa Barbara California Operations) using a similar setup except with reduced input power (≈ 1 milliwatt/cm^2). Those data are also summarized as Data Set 2 in Table II. Further independent measurements on fourteen F411 MCPTs were made at ITT's electrooptic Devices Laboratory (Ft. Wayne, Indiana) with similar results tabulated as Data Set 3 in Table II.

The various transmission data range from 10^{-4} to 10^{-9}. Excluding low and high transmission values, we can probably conclude that, to an order of magnitude accuracy, the typical ITT MCPT optical transmission is from 10^{-5} to 10^{-7} and the Varo MCPTs appear to have 10x better attenuation.

The transmission from phosphor to photocathode was also measured on some samples. There is a stronger angular dependence in this direction with a few degrees (approx. 15°) from normal (light source axis perpendicular to MCPT photocathode) causing as much as two orders of magnitude change in transmission. For the perpendicular orientation, the majority of samples (8 of 12) showed lower attenuation (2x to 10x) in this direction.

Experimentation with various thicknesses of aluminum oxide phosphor coating to improve attenuation of feedthrough without sacrificing too much gain was performed at ITT. The results are summarized in Table III. For SITVs, the side of the silicon target that faces the image beam (photocathode side rather than electron gun side of SITV) has a thin (hundreds of angstroms) chromium layer which serves as a semi-opaque light barrier to minimize sensitivity to photons. Layer thicknesses were measured at GE during manufacture using a quartz crystal oscillator and analyzing resonances. The data for 3 SITVs is in Table III.

Table III. MCPT and SITV transmission vs target coating thickness

	Approximate Thickness (Å)	% transmission (Coating+tgt+fo coupler)	dead voltage	remarks
Normal	--	3×10^{-3}	3 KV	--
1st attempt:	--	4×10^{-4}	-	Al lifted upon application of HV
2nd attempt:	--	6×10^{-4}	3.4 KV	Used on SN14-311/4 R&D MCPT.
3rd attempt:	--	1.5×10^{-5}	3.7 KV	Not yet tested in MCPT geometry.
SITV-1	< 100	≈ 20%	< 3 KV	
SITV-2	200	2 to 4%	3 KV	- -
SITV-3	700	< 1%	3.5 KV	- -

The overall SITV transmission,[2] measured by removing high voltage from the image section while illuminating the photocathode with CW light and observing silicon target video, indicated optical attenuation from 3.2×10^4 to 2×10^5 for five units. Three SITVs with chromium in the 600 to 800 Å range gave attenuation in the 10^6 to 10^7 range. The possibility of externally coating MCPT output (phosphor) fiber optic couplers with narrow band transmission filters spectrally matched to the P-20 phosphor to suppress feedthrough at other wavelengths is under investigation. Various thicknesses of high index of refraction metallic materials including aluminum oxide and cadmium sulfide and low index of refraction dielectrics such as magnesium fluoride are being investigated to evaluate possible sandwich (metal-dielectric-metal) thicknesses before resolution losses become too severe.

Photoemission suppression

The phosphor brightness as a function of photocathode-to-microchannel plate voltage was measured using a standard light source of variable intensity and a intensifier-based optical multichannel analyzer (Princeton Applied Research Model #OMA-3). The transfer curve for bias voltages in the range from -50 to +50V is shown in Fig. 4. The zero to -50V portion corresponds to reverse bias and the zero to +50V corresponds to forward bias. For ideal shutter control, the reverse bias range should provide complete suppression of photocathode emission while the forward bias should produce a linear gain function.

Small leakage emission at small reverse voltages (≈ -25 to 0V) and maximum MCP gain was observed from either Varo or ITT units. This was unexpected because the energy range of incident visible photons is 1.5 to 3.2 eV. Our earlier work[3] does show some gate transmission at near zero bias, albeit with reduced performance. For small forward voltages (≈ 0V to +6V) the MCPT is undergoing a transition phase associated with establishing sufficient electric field across the photocathode-to-MCP$_{in}$ gap to allow penetration of photoelectrons into the MCP. Slightly larger voltages (≈ +15V to +20V) are required for proximity focusing to be established. Beyond +20V, gain increases linearly with voltage and resolution shows only a weak dependence on voltage.

Tests were performed to measure the effectiveness of currently used MCPT bias circuitry (Fig. 3) in suppressing photocathode emission. The reverse bias potentiometer, R_4, provides a voltage range from 0 to -50 volts between photocathode and microchannel plate input to keep the MCPT quiescently shuttered off. For gating the MCPT on, a forward-biasing negative 80V 1.5 ns FWHM gate pulse (Fig. 5) is AC-coupled through C1 and C2 to the photocathode. The algebraic difference between the gate pulse amplitude and the static reverse bias is the effective forward bias voltage as indicated in Fig. 6.

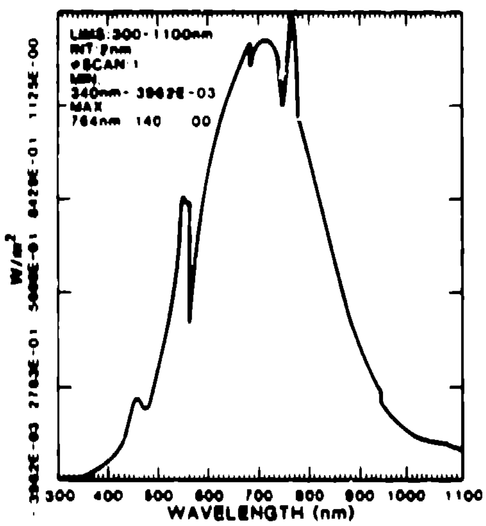

Fig. 2. Spectrum of CW source used for opacity experiments.

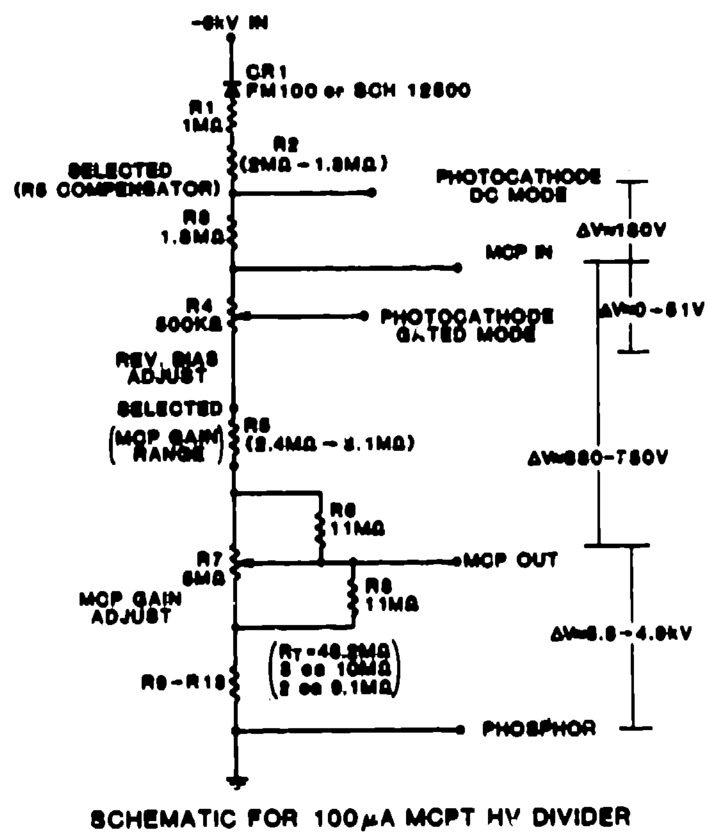

Fig. 3. High voltage divider circuit used for biasing MCPTs. Voltages shown are measured values under load with MCPT in the dark.

Fig. 4. MCPT phosphor optical energy versus photocathode-to MCP_{in} bias for constant input intensity.

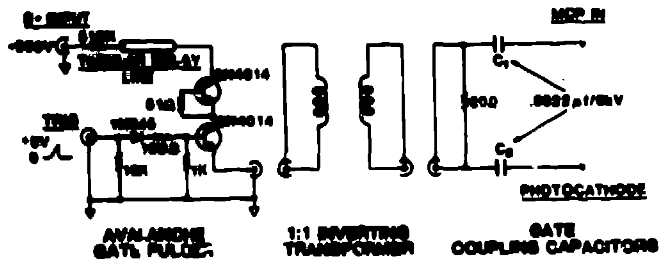

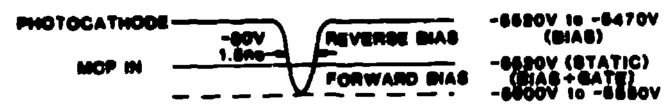

Fig. 5. Avalanche gate pulser for gating MCPTs

Fig. 6. Biases established by combining divider and pulser circuits.

Two standard configuration MCPTs, ITT F4111 and Varo 5722-II were operated in the AC or gated mode (non-gated phase) with high voltage applied but with no gate pulse so the tube should be shuttered off over the range of reverse bias provided by R_4. The MCPT was then strobed with a high intensity short duration Xenon flash (see Fig. 7) and the phosphor signal was recorded by an Sb_2S_3 FPS vidicon fiber optically coupled to the MCPT. The series of video scan-line photographs in Fig. 8 show that when the MCPT and phosphor have voltages across them (both are active and ready to provide gain for any electrons that reach them) the leakage photoemission is amplified even though the MCPT is assumed to be off and no gate pulse is applied. The Varo unit appeared to be less effectively biased (allowed more leakage photoemission) than the ITT unit, as indicated by the larger ND filters required to give the same amplitude as for the optical feedthrough signal.

Because of gain, the difference in gated or DC mode signal amplitude vs optical throughput with no HV is greater (by an amount equal to the gain of the tube) than the optical shutter ratio. This is also shown in Fig. 8. For typical ITT and Varo units, the DC mode signal for Max MCP gain is from 10^{10} to 10^{11} stronger than the optical feedthru. For these same MCPTs, the optical shutter ratio is from 10^6 to 10^7.

The gain dependence on reverse bias was further analysed using the setup shown in Fig. 9. An EG&G 550 radiometer was used to measure phosphor brightness at the center of the optical gate at several reverse bias voltages with fixed gate amplitude (refer to Figs. 5-7 for clarification of actual division between forward and reverse biases). The plots for two different MCPTs, ITT SN 14-311/4 and Varo SN 324054 are found in Fig. 10. Again, the ITT unit appears to be more effectively biased off than the Varo unit at lower reverse-bias settings.

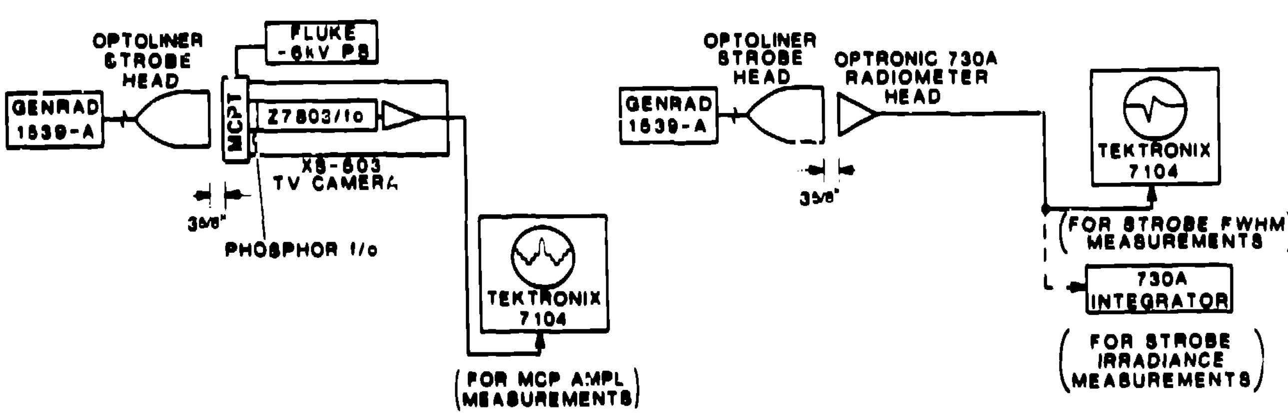

PHOTON/ELECTRON SHUTTER RATIO TEST SET-UP

Fig. 7. Setup for photocathode leakage emission experiment. The light source is a General Radio Strobe, Model 1539-A. The vidicon coupled to the MCPT phosphor measures phosphor signal induced by photoelectrons which are not suppressed by the reverse bias.

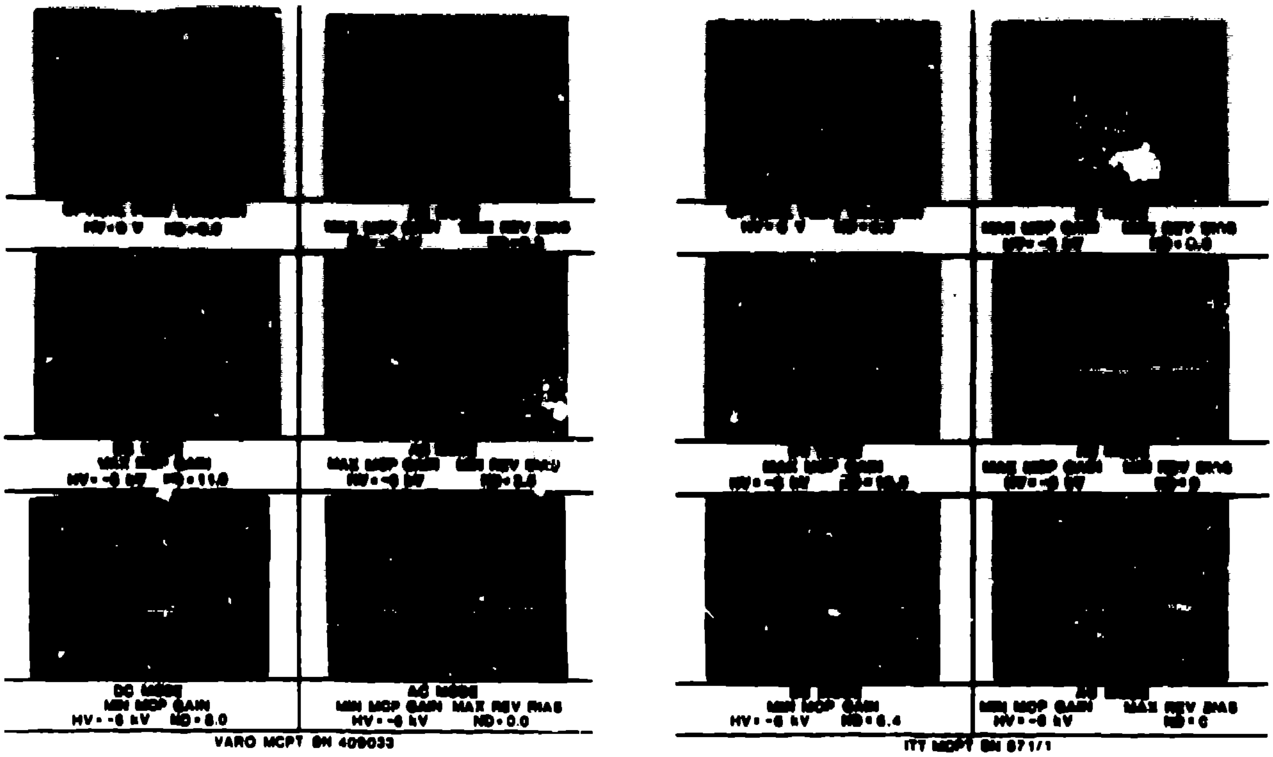

a b

Fig. 8. Non-gated leakage emission versus reverse bias for two MCPTs. Part a, for a Varo MCPT shows poorer suppression than for ITT sample, part b.

Dynamic Shuttering

Static shutter ratios are measured by first obtaining a given signal amplitude in the DC mode for a known optical intensity. Then the shutter tube is operated in the gated (AC) mode but in its non-gated phase and the input intensity is increased until the same signal amplitude is obtained. The ratio of the two intensities, corrected for the difference in AC and DC gains, is the shutter ratio.

A more rigorous measurement was made which mapped the transmission behavior immediately before and after optical gate termination. The setup for this experiment is in Fig. 11. A PAR model LN-102 dye laser excited by a PAR model LN-100 nitrogen laser emits 500 ps FWHM pulsed light which travels over an optical path of about 10 meters in air. The dye used was C481 with a peak wavelength of 480 nm. A long focal length lens focused the laser beam on the photocathode of the MCPT. Scattered light from this lens was used to saturate an RCA 8570 photomultiplier which triggered the gate pulser through an adjustable cable delay. The gate pulse (and therefore the MCPT optical gate) was adjustable from several tens of ns after to about 2ns before the light pulse. First, the delay was adjusted so that the light pulse was coincident with the peak of optical gate and ND filters were inserted in the beam path until a minimum detectable signal was observed. The delay was then varied, "walking" the optical gate either side of the light pulse and ND filters were removed until the minimum detectable signal was again observed. In this manner the optical power extinction ratio of the MCPT was measured at several points in time relative to the peak of the optical gate. The data for one ITT and one Varo MCPT are plotted in Fig. 12. A long fluorescence tail (tens of ns duration at $\approx 10^{-6}$ of peak intensity associated with the main dye pulse is shown at the leading edge of the optical gates. In our normal procedure for characterizing gating speed[1-3] only the top three decades of extinction are used because of typical 10^2 to 10^3 dynamic range of the cascaded MCPT/vidicon. Based upon that method, optical gate widths of $\approx$ 3ns would be determined for these MCPTs. However, for shuttering against light widths > optical gate widths, the total dynamic shutter ratio must be included to accurately define the total optical gate width.

Additional measurements using a radiometer in lieu of the SIT vidicon were taken throughout two MCPT optical gates at various bias levels. Referring to Fig. 9 for setup details, a new gate Sequence Analyser[4] (laser diode/MCPT gate pulser synchronizer) was used to generate repetitive (2 KHz) optical gates. The radiometer readings were recorded at 1ns

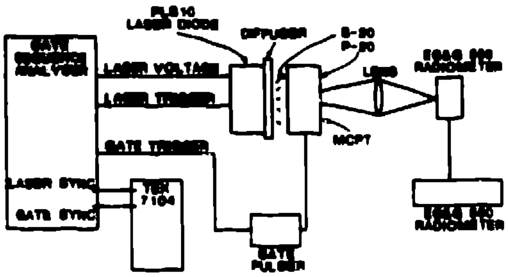

Fig. 9. Setup for measuring MCPT gain profiles throughout an optical gate sequence as functions of gate time and gate bias.

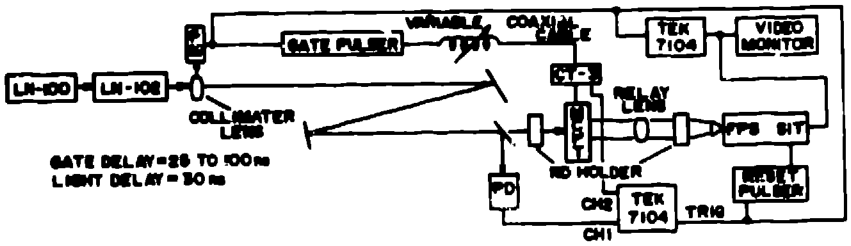

Fig. 11. Dynamic Shutter ratio experimental setup.

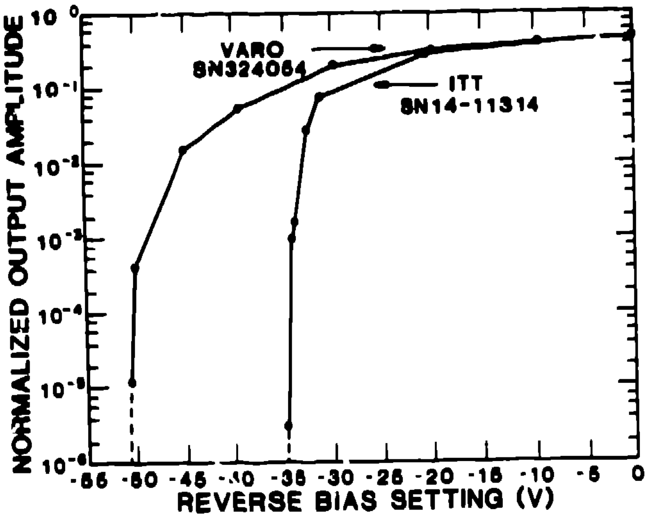

Fig. 10. MCPT gain dependence on reverse bias.

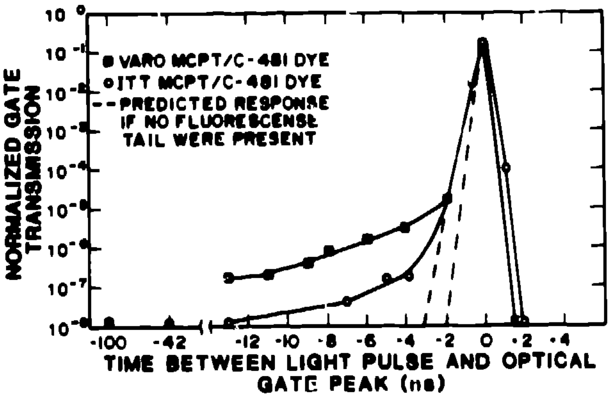

Fig. 12. Shutter ratio relative to center (zero) of optical gate.

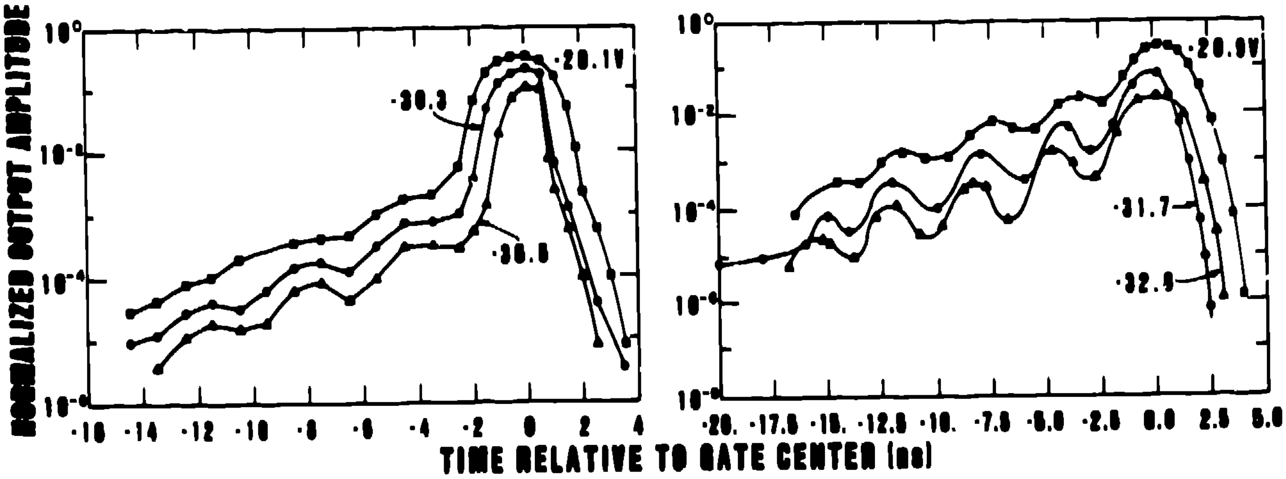

Fig. 13. Gain relative to center (zero) of optical gate for two MCPTs at three reverse bias levels.

increments. The data obtained was normalized using a computer program. Before normalization a DC to AC gain measurement was made. This was done and all data was normalized such that the DC output is 1.

The data (Fig. 13) shows similar widening of the optical gate at low signal amplitudes. The ringing is attributed to electrical reflections from poor gate pulse termination. The greater sensitivity of the SIT vidicon permitted tracking the gate transmission at lower phosphor emission levels. Also, the LN-102 dye laser provided more optical power/pulse than the PL3-10 laser diode resulting in the longer plot in Fig. 12.

Conclusions

Optical feedthrough establishes the lower limit of usefulness for MCPTs and SITVs when the light pulse is equal to or shorter than the optical gate. For light pulses longer than the gate, the feedthrough signal integrated over the time duration of the light compared with the gated signal integrated for the gate duration gives a first approximation effect of feedthrough.

Leakage photocathode emission establishes another lower-level threshold. Because of the sharing effect (of static and gated voltages) between reverse and forward biases, signal levels within the gate vary non-linearly as functions of (1) gated gain due to increasing forward voltage and (2) leakage gain from simultaneously decreasing reverse voltage. Outside the gate, leakage emission amplification is a function of reverse bias.

Acknowledgments

The authors wish to thank John Bujnosek of Los Alamos National Laboratory, Vanner Holmes of EG&G Los Alamos, for help in measurements, Terry Davies and Melvin Nelson of EG&G Santa Barbara for support in electrooptic measurement apparatus, Teresa Martinez of EG&G Los Alamos for image processing support, and John Cuny and Phillip Taylor of ITT for help in opacity measurements and phosphor coating experiments.

References

1. Yates, G. J., Nanosecond Image Shuttering Studies at Los Alamos National Laboratory, IEEE Transactions on Nuclear Science, Vol. NS-31, No.1, pp. 484-489, February 1984.
2. Yates, G. J., et al., A High Resolution SIT TV tube for Subnanosecond Image Shuttering, Los Alamos National Laboratory Report, LA-9771-MS, September 1984.
3. King, N.S.P., et al, Nanosecond Gating Properties of Proximity-focused Microchannel-plate Image Intensifiers, Proceedings SPIE, Vol. 288, pp. 425-433, 1981.
4. Pagano, T.S., et al, Picosecond Semiconductor Lasers for Characterizing High Speed Image Shutters, Proceedings SPIE, Vol. 569, paper 569-29, 1985.